JOURNAL OF MATERIALS SCIENCE 18 (1983) 3686–3694

Microstructural studies of the hydration products of three tricalcium silicate polymorphs

H. R. STEWART, J. E. BAILEY
Department of Metallurgy and Materials Technology, University of Surrey, Guildford, UK

Tricalcium silicate (C_3S), the major phase of Ordinary Portland Cement (OPC), occurs in several polymorphic forms depending on the amounts and types of impurity ions present. The hydration products of triclinic, trigonal and monoclinic C_3S samples have been studied for a comparison with the silicate hydration products of OPC, using TEM and SEM. In the early stages, less than one day, there are distinct differences observed between the products on the surfaces of grains of different crystal structure but later all three appear similar. This suggests a common mechanism of hydration at later times, irrespective of structure, but the influence of the foreign ions in the first few hours is significant.

1. Introduction

Although many features of the hydration reaction of Ordinary Portland Cement (OPC) and morphology of the products have been recognized for many years, and despite the appearance in the literature of increasing amounts of chemical and analytical data, the mechanism of hydration remains obscure [1, 2].

Of the four main phases C_3S, βC_2S, C_3A and C_4AF,* the calcium silicates constitute around 70 to 80% and a study of their activity alone has often been considered to give a good indication of how the material as a whole behaves. Furthermore, both the silicates give very similar hydration products; an amorphous calcium silicate hydrate gel (C–S–H) of apparently indefinite composition, and crystalline calcium hydroxide. However, there is a significant difference in the rates of hydration, the C_3S attaining considerable strength much earlier than βC_2S. As C_3S is the major component of OPC it is the obvious first choice as a model compound for a study of cement hydration. A comprehensive study of the development of the microstructure of hydrating C_3S has been made by Jennings *et al.* [3] and they have suggested a new classification of C–S–H morphologies, in addition to that of Diamond [4] for the silicate phases of OPC.

The crystal structure of C_3S was investigated by Jeffery [5] and the trigonal pseudostructure which he proposed is a good approximation to the true structure [6]. The existence of seven different polymorphs between ambient temperature and 1100° C has been recognized [7, 8].

$$T_I \underset{}{\overset{600^\circ C}{\rightleftharpoons}} T_{II} \overset{920^\circ C}{\rightleftharpoons} T_{III} \overset{980^\circ C}{\rightleftharpoons} M_I \overset{990^\circ C}{\rightleftharpoons} M_{II} \overset{1060^\circ C}{\rightleftharpoons} M_{III} \overset{1070^\circ C}{\rightleftharpoons} R$$

Each transformation involves only minute displacements of structural groups. At normal temperatures only the T_I form is found but the presence of foreign ions, such as magnesium, aluminium and transition metal ions which form solid solutions with C_3S, may stabilise the other polymorphs. Replacement of Ca^{2+} or Si^{4+} or both may occur depending on the size and charge of the impurity ion.

OPC can contain any or all of the three types of C_3S structure, triclinic, monoclinic and trigonal, depending on the amounts and types of ions able

*C = CaO, S = SiO_2, A = Al_2O_3, F = Fe_2O_3, H = H_2O.

0022–2461/83 $03.00 + .12

to form solid solutions. Normally, however, the composition is such that the monoclinic form predominates [9] and the triclinic form is rarely found except in mixes with few impurities. Nevertheless, hydration studies of C_3S reported in the literature most frequently involve pure triclinic C_3S which may therefore not be the best model for silicate hydration in OPC. Hence, in this study three different polymorphs of C_3S have been investigated and the course and rate of reaction and morphology of the products obtained compared with those of the silicate phases of OPC.

2. Experimental details

The three C_3S polymorphs and OPC studied were provided by Blue Circle Industries. The monoclinic sample (MC_3S) was magnesium stabilized, the trigonal form (RC_3S) contained 0.6% fluorine and 1.5% alumina and the triclinic sample (TC_3S) contained no foreign ions. The free lime content of the samples was 0.3% after four firings at 1400° C with intermediate grinding. It should be stressed that these modified samples are only examples of some of the different crystal structures which can be obtained, and may not be typical of a range of materials with the same nominal structure. For comparison, typical OPC batch 112 was used. The hydration reaction profile with time was monitored by conduction calorimetry at Blue Circle Technical Research Division, Greenhithe and traces for each sample are shown in Fig. 1 with corresponding data in Table I.

Transmission electron microscopy (TEM) samples were prepared at a water/solid ratio of 0.5 using the method of Bailey and Chescoe [10].

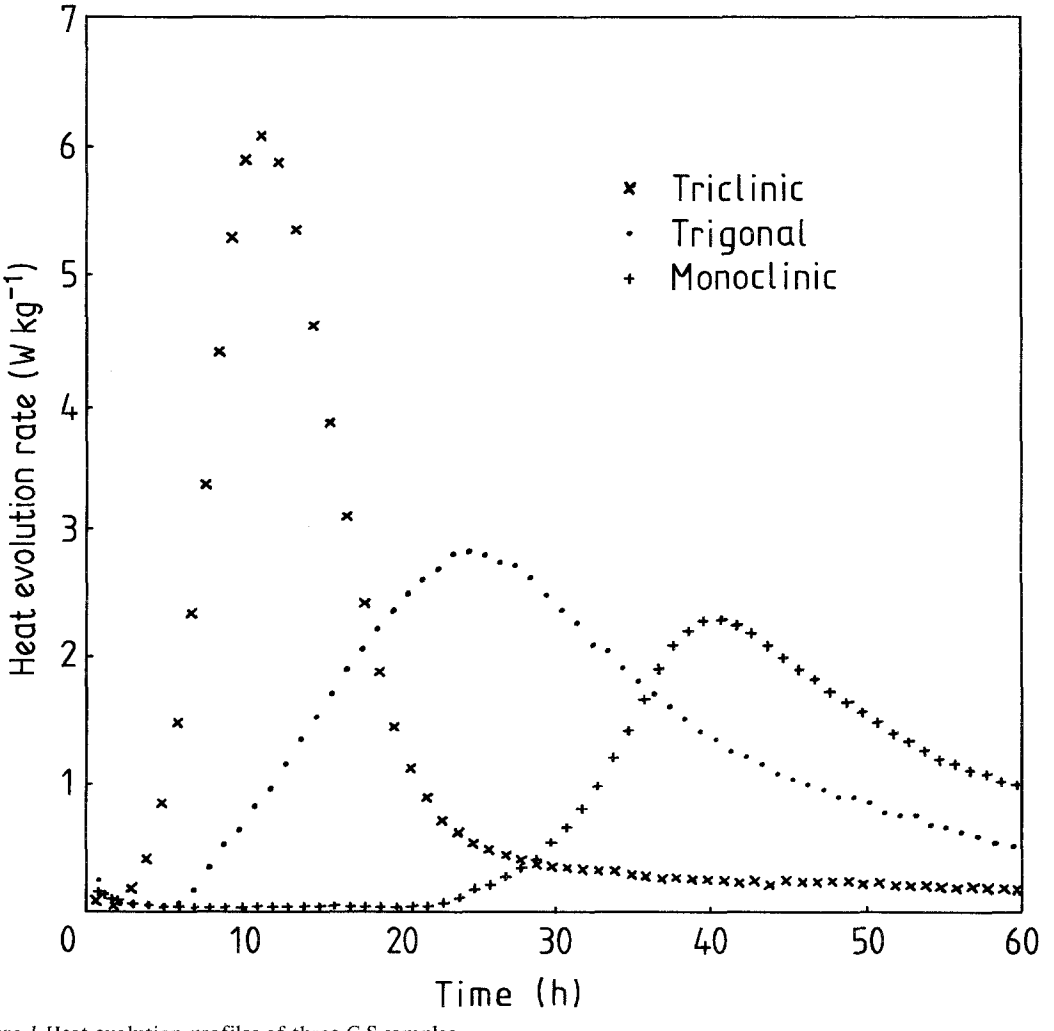

Figure 1 Heat evolution profiles of three C_3S samples.

TABLE I Conduction calorimetry data for three C_3S polymorphs and OPC

Sample	Time of end of induction period (h)	Time of maximum heat evolution (h)	Heat evolved at maximum ($J g^{-1}$)	% hydration at maximum
MC_3S	24	40.5	67	13
RC_3S	8	25	109	22
TC_3S	3	11.5	92	18
OPC	1	7	59	

The series of micrographs in Figs. 2, 3 and 4 illustrate the course of the hydration reaction and products formed. These observations are best discussed in relation to the degree of hydration that has occurred as evidenced by the calorimetry curves for each polymorph. This is estimated from the integrated calorimetric data on the basis that 100% hydration corresponds to a total heat evolution of $503 J g^{-1}$ [11]. In the earlier stages there are morphological differences between the hydration products of the different polymorphs but at later stages all three have a similar appearance. In the monoclinic sample at early ages the characteristic feature of hydration, as clearly seen in Figs. 4a and b is a thin crumpled sheet morphology surrounding the particles, persisting beyond the time of maximum heat evolution. The triclinic and trigonal samples contain needle-like outgrowths (Figs. 2c and d, and 3a and b) randomly located over the surface and these increase in concentration with time.

In addition to the main characteristic hydration products formed, a fine silicon-rich deposit is observed in each specimen in the first few hours of hydration (see Fig. 2b) and later loose foils are seen which appear to have formed by a through solution growth mechanism (Fig. 2e). Also during the first few minutes of hydration, in freshly prepared samples, a few isolated bursts of calcium-rich outgrowths, contaminated by silica, are seen, for example, see Figs. 2a and b. These outgrowths are similar in form but larger than C–S–H needles produced in the early stages. Analysis confirms their different composition and electron diffraction shows they have some degree of crystallinity, depending on the amount of silica incorporated. These structures are most likely associated with the hydration of free lime, an impurity which is difficult to eliminate during synthesis. Elements used to stabilize the different polymorphs give rise to their own hydration products. Thus a few $Mg(OH)_2$ crystals are found in the monoclinic sample and various hexagonal plate structures containing aluminium are present in the trigonal sample with C–S–H growing around them. It is impossible to say at this stage whether these originated from unreacted material in the firing cycle or if the elements have been preferentially removed from the C_3S on hydration.

Although significant levels of aluminium were detected in the C–S–H in the trigonal sample, consistent with the concentration in the raw mix, only a trace of magnesium was detected in the monoclinic case.

The early hydration products described above are seen up to times corresponding to the maximum heat evolution peaks of the calorimetry curves and thereafter a transition to late hydration product occurs. In each case the late products have a crumpled foil morphology extending outwards from the surface and the three samples are visually indistinguishable (Figs. 2f, 3c and 4d).

The hydration behaviour of the calcium silicate phase of OPC and the development of the microstructure was compared with the C_3S pastes. X-ray diffraction analysis confirmed that the major form of C_3S present was monoclinic. None of the flaky sheet early hydration product observed in the pure monoclinic sample was obtained. At all stages the silicates in OPC (Figs. 5a, b and c) resembled most closely the triclinic C_3S both in reaction rate and morphology of the products.

3. Discussion

There is no real evidence in the literature that the order of reactivity of C_3S polymorphs depends on the type of crystal structure alone and this is understandable considering that the same type of structure can be produced by several methods. Harada *et al.* [12] found that in the initial stages, after one day, the trigonal form reacted fastest, then the triclinic and then the monoclinic, but the order changed at later times. In contrast Yamaguchi *et al.* [13] found that triclinic and monoclinic samples reacted at the same rate. Thermodynamic calculations suggest that the monoclinic

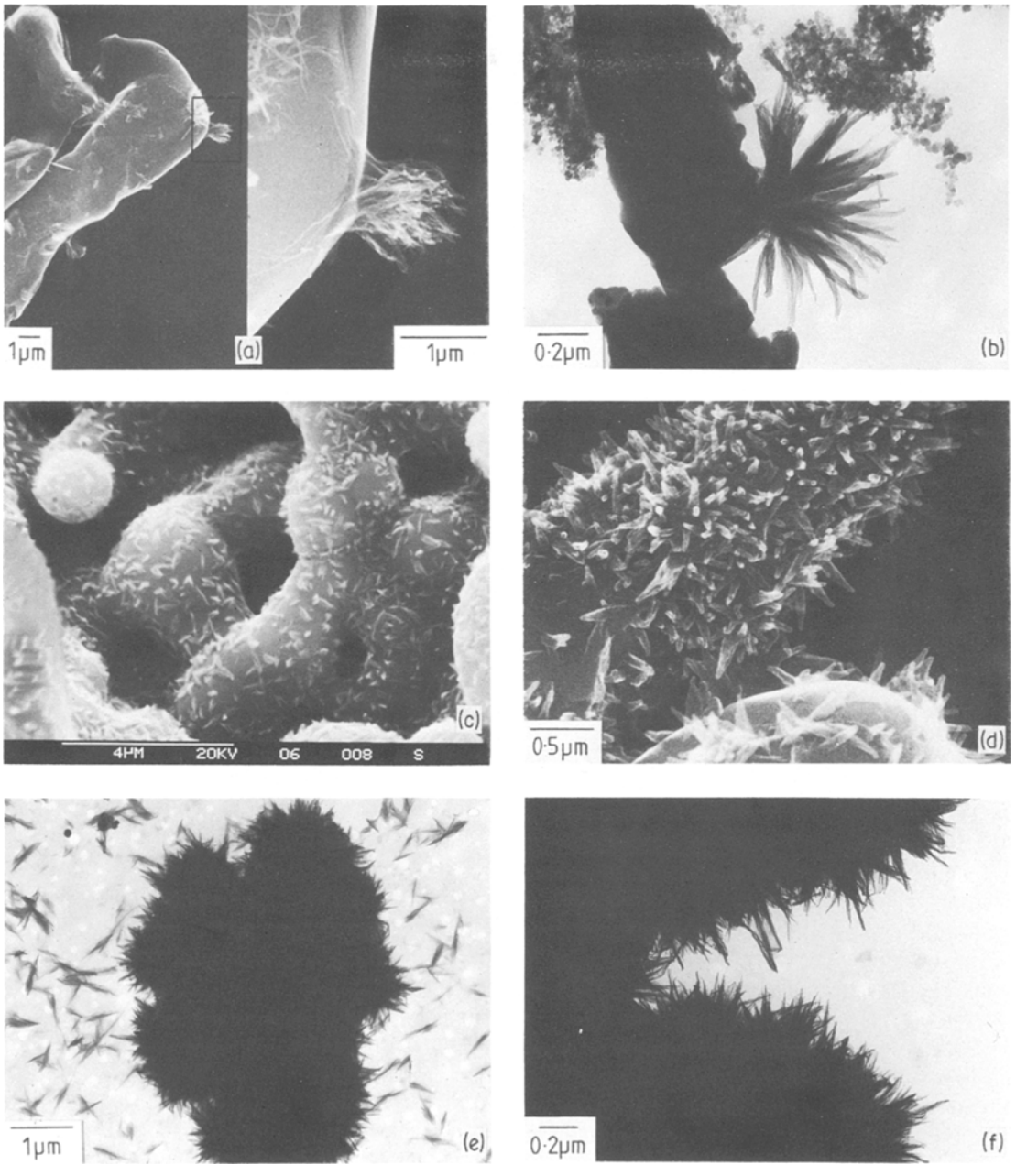

Figure 2 Development of the microstructure of triclinic C_3S (a) 30 min, (b) 30 min, (c) 6 h, (d) 12 h, (e) 24 h, and (f) 28 days.

form should be more reactive than pure TC_3S since substitution of Ca^{2+} by the smaller Mg^{2+} in the lattice gives a less stable and hence more reactive MgO_6 group. However this was not found by Valenti *et al.* [14] who studied the degree of hydration of several alites as a function of time. Their results clearly showed that in the early stages, pure C_3S reacted faster than a sample containing 1% Al_2O_3. The rate of reaction depends not only on the type of substituting ion but also on its concentration as demonstrated by Thompson *et al.* [15] for monoclinic C_3S. An increase in MgO content from 1.45 to 2% caused marked changes in the heat evolved at 35 h, reflecting different reactivities. Aldous [16, 17] has investigated the effect of various combinations and concentrations of aluminium, magnesium, fluorine and sulphur on alite structure and reaction profiles,

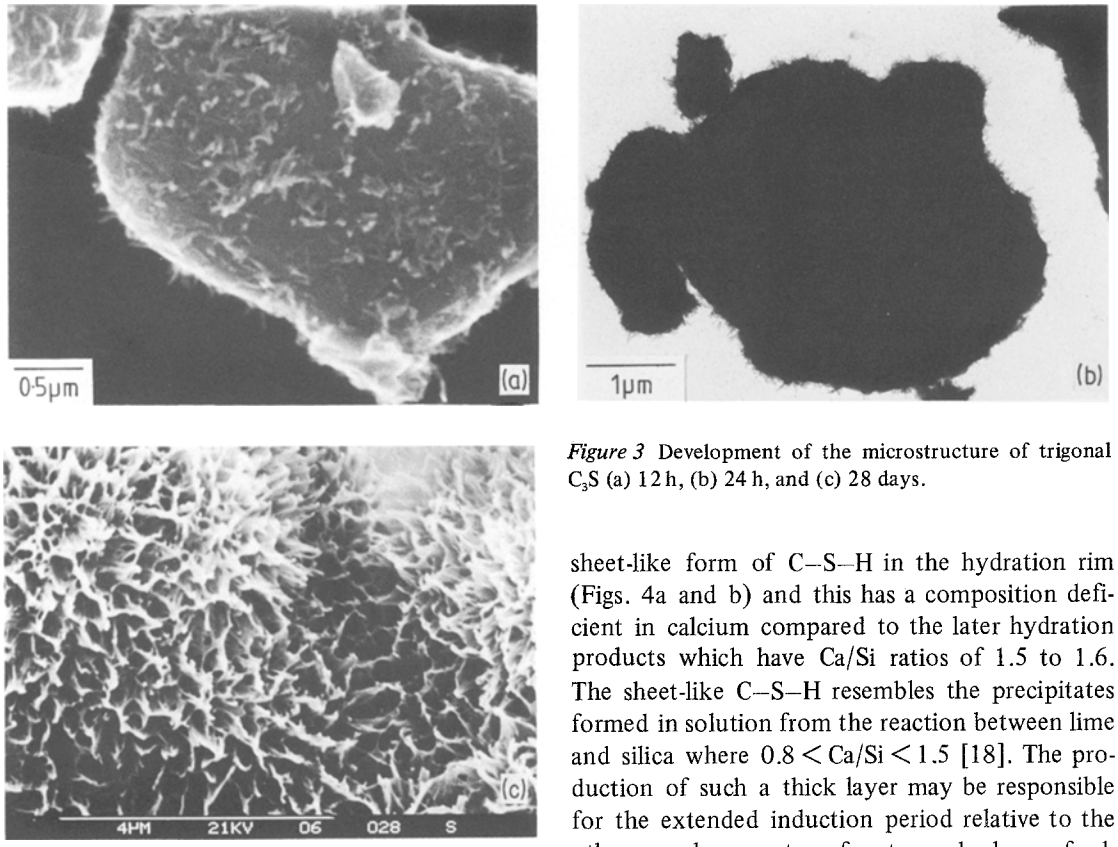

Figure 3 Development of the microstructure of trigonal C_3S (a) 12 h, (b) 24 h, and (c) 28 days.

and a wide range of effects are thus produced. In both the previous studies there was enhanced reactivity of samples stabilized on the transition between two polymorphs which is to be expected for such high energy intermediate crystal structures. The basic reasons for the differing rates of reaction are therefore uncertain and a great deal more work must be done to resolve this problem. However, since the reaction profiles all show the same features it is interesting to consider the variation in morphology between C_3S polymorphs at the same stage of reaction, e.g. end of the induction period, or at the time of maximum heat evolution. For convenience the calorimetry curve is divided into five regions as shown in Fig. 6.

Stage I involves an initial rapid reaction which gives off a burst of heat. In the second stage, the triclinic and trigonal polymorphs have the same reaction products but different reaction rates, and the monoclinic C_3S is distinctly different. It is therefore tempting to suggest a reaction mechanism which is dependent on the impurity ions and crystal structure or perhaps defects in the structure. In the monoclinic case there is a diffuse sheet-like form of C–S–H in the hydration rim (Figs. 4a and b) and this has a composition deficient in calcium compared to the later hydration products which have Ca/Si ratios of 1.5 to 1.6. The sheet-like C–S–H resembles the precipitates formed in solution from the reaction between lime and silica where $0.8 < Ca/Si < 1.5$ [18]. The production of such a thick layer may be responsible for the extended induction period relative to the other samples as entry of water and release of calcium ions are retarded. Thermodynamic considerations would suggest that the magnesium ions on the C_3S surface might react to form M–S–H in preference to C–S–H production in the very early stages, but analytical evidence has failed so far to show magnesium enrichment in the sheet-like hydration product. In the triclinic and trigonal samples the surface remains smooth as in Fig. 2a, showing little evidence of reaction except for a few isolated outgrowths (Figs. 2a and b) and lifting of a thin surface film, until the end of the induction period.

In stage III the concentration of the sheet like C–S–H builds up steadily in the monoclinic sample but even at the time of the maximum heat evolution the degree of hydration is significantly lower than for the other two samples as the data in Table I demonstrate. On the triclinic and trigonal sample grains, a different type of needle-like outgrowth of about 0.5 μm in length appears, generally at shallow angles (Figs. 2c and d, and 3a and b). These C–S–H products increase in number steadily with time until at the maximum heat evolution peak the original surface is just covered (Fig. 2d). At this point the degree of hydration is

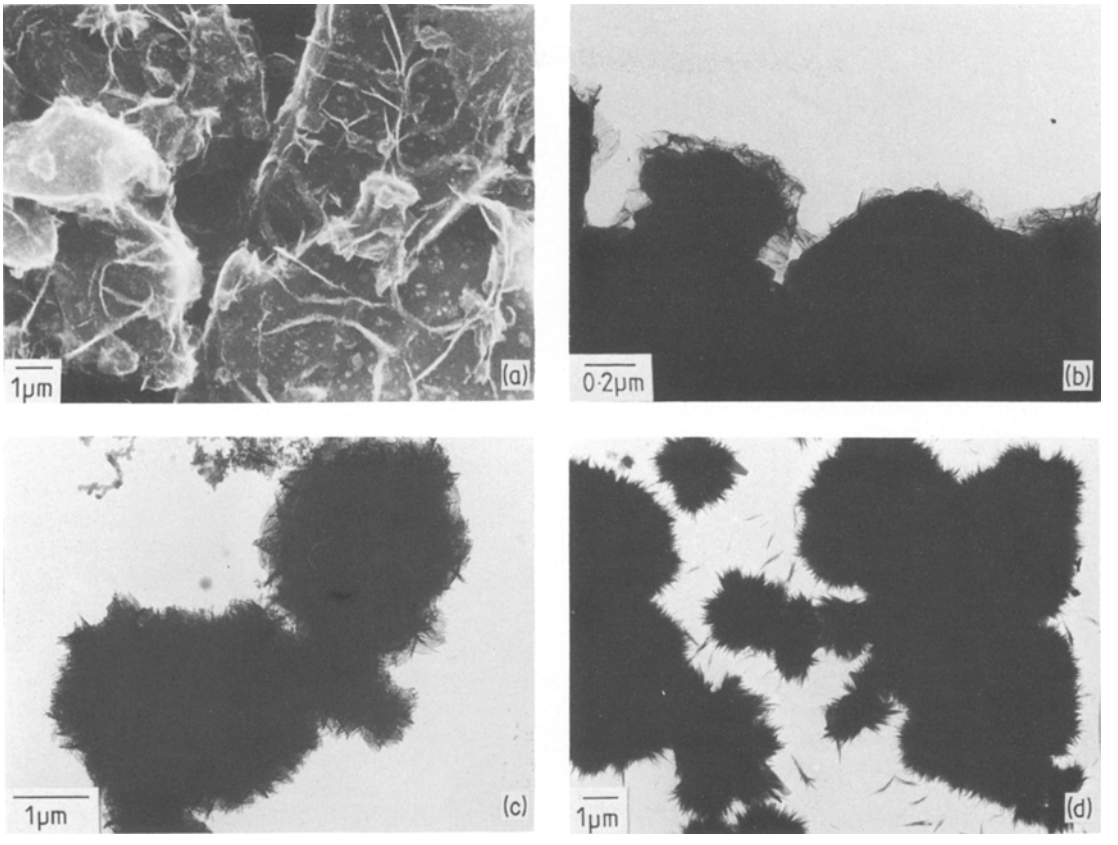

Figure 4 Development of the microstructure of monoclinic C_3S (a) 24 h, (b) 48 h, (c) 7 days, and (d) 28 days.

20%. A simple calculation has been carried out to determine whether or not the event of achieving surface coverage with such outgrowths is consistent with the calorimetric data.

Assuming a conical shaped outgrowth of base radius 0.1 μm and length 0.5 μm, and a surface area of C_3S of 3000 $cm^2 g^{-1}$ then the volume of a monolayer of outgrowths is 5×10^{-2} cm^3 per gram of C_3S. Allowing for the different densities of anhydrous C_3S (3.2 g cm^{-3}) and C–S–H gel (2.25 g cm^{-3}) then the degree of hydration 15%. This is lower than the value of 20% suggested by calorimetry but many factors could account for this. For example it is likely that a layer beneath the outgrowths is somewhat hydrated and it is calculated that such a layer would need to be only 0.6 μm thick to make up the difference. Also the calculation assumes that all the C–S–H is on the grain surfaces and that none precipitates remote from surfaces. Nevertheless, this result tends to suggest that to a first approximation at the time of maximum heat evolution when around 20% of the C_3S is hydrated, the majority of the C–S–H reaction products are located on grain surfaces in the form shown in Fig. 2d and are not the result of through solution precipitation.

Furthermore it is suggested that the complete covering of the surface by outgrowths is responsible for the subsequent decrease in rate of hydration as the access of water to the anhydrous C_3S and the deposition of further C–S–H are restricted.

The origin of these sharp, well defined and uniform outgrowths is difficult to ascertain as each contains a substantial amount of material and yet the particle surface in the immediate vicinity appears undisturbed and continuous up to the needle base. In the early stages, the distribution of reactive sites appears random and on a scale which is much greater than can be accounted for at the atomic or molecular level. Neither does it seem that the production of any single outgrowth influences the subsequent location of its neighbours. It is possible that slight compositional variations may be present but unlikely that these would be so evenly dispersed and the fact that the

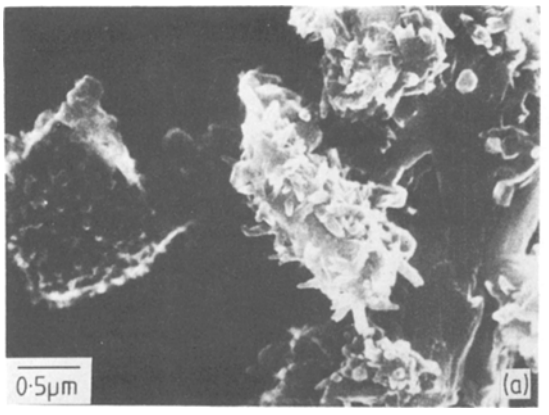

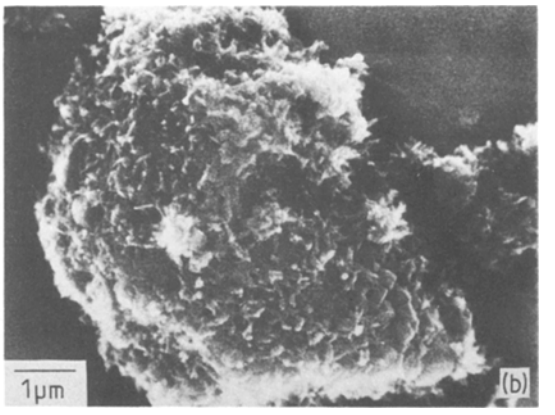

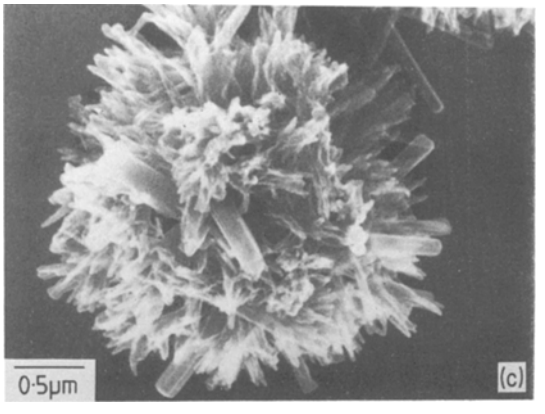

Figure 5 Development of the microstructure of the silicate phases of OPC (a) 4 h, (b) 6 h, and (c) 24 h.

triclinic and trigonal polymorphs show the same behaviour despite aluminium and fluorine impurities in the latter tends not to support this suggestion for the existence of preferred reaction sites. Physical defects may be responsible, but nevertheless the microstructural evidence indicates that ultimately each site may be similarly activated, as the entire surface eventually becomes covered by identical needles. Analogies with the growth of silicate gardens have led to the proposal of a membrane/osmosis model of hydration [19] whereby osmotic pressure under the surface film of C–S–H is considered to cause its rupture. The nature of the rupture phenomenon will depend upon a number of factors, for example if the volume of the osmotic cell is very small, as is most likely, the pressure difference will be rapidly reduced when a rupture occurs in the C–S–H film. This may perhaps explain the limited size of the observed needle-like outgrowths and the steady increase in the number of them with time. Furthermore, the mechanism by which the initial C–S–H film ruptures will depend on the rheological properties of the film. It is hoped to expand upon this model, after further experiments, at a later stage.

If it is assumed that the cementing action is the result of overlap and intergrowth of the needle-like hydration products then a calculation of the expected volume increase in C_3S particles on hydration to C–S–H is relevant. The following reaction can be considered to occur.

$$2C_3S + 6H \rightarrow C_3S_2H_3 + 3CH.$$

The minimum water/solid ratio required is therefore 0.24 for 100% hydration. From the data in Table II it is clear that 1 g of C_3S plus 0.24 g of water, which occupy 0.55 cm^3 of paste, will produce 0.75 g of C–S–H (0.33 cm^3) and 0.49 g of CH (0.22 cm^3). If the CH precipitates in the original water volume only, then the volume occupied by C–S–H is only 6% greater than the original C_3S volume. For a typical particle of diameter 10 μm this can be achieved by an increase in radius of 0.1 μm. This corresponds to a distance less than the mean length of C–S–H needles, so assuming a suitable geometry is attainable the production of a monolayer of needle-like outgrowths on the particle surface is more than sufficient to produce an aggregated mass without significant mass transport of the calcium and silicate ions forming the C–S–H. For a more realistic water/solid ratio of 0.3 the extra water is contained in pores and in C–S–H gel, thereby reducing its density but again, very little volume increase is necessary.

TABLE II

Material	Mwt (g mol^{-1})	Density (g cm^{-3})
C_3S	228	3.2
H	18	1.0
$C_3S_2H_3$	324	2.25
CH	74	2.25

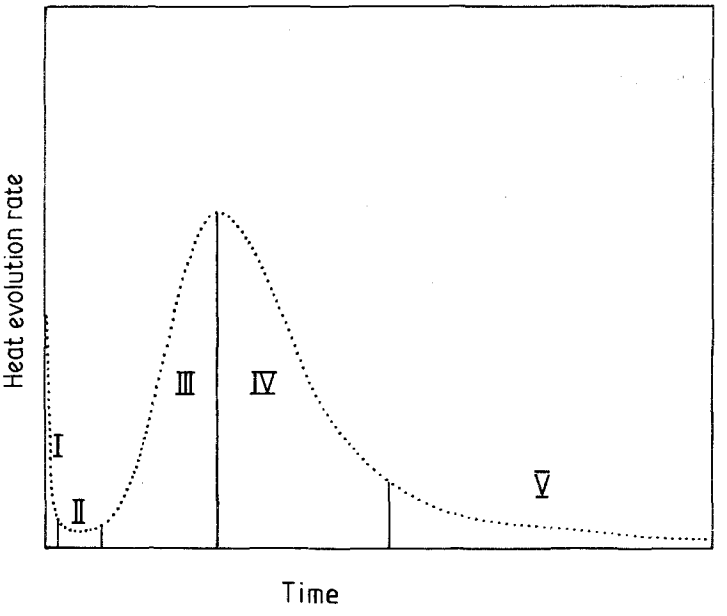

Figure 6 Classification of the hydration stages of C_3S paste.

Thus the production of needle-like outgrowths forms a framework which bridges the particles and hydration products are subsequently laid down within its confines. This mode of precipitation of C–S–H allows the gel to extend further into space than would a simple radial expansion for the same degree of reaction, and by interconnection of needles allows a greater surface area of interaction between hydrating particles. The mechanism accounts for the relatively high rate of gain of early strength of pastes when the degree of hydration is low (less than 40%).

At the end of stage III the C_3S surface is covered by needle-like hydration product and subsequently hydration proceeds towards the centres of the grains. The expansion produced leads to infilling of the space between needles with a thin sheet-like form of C–S–H as shown in Figs. 2f and 3c, and considerable densification of outer product results. Little change is observed in the external hydrates thereafter. In the monoclinic sample in stages IV and V the sheet like material begins to convert gradually to a more needle like morphology, as seen in the other two samples, until after several days it is indistinguishable from them. It is remarkable that the different structures seen in the early stages transform to essentially the same form at a later stage. This demonstrates the dynamic nature of the system and slow approach to equilibrium, with ionic species remaining mobile for a considerable length of time until each paste eventually attains virtually the same minimum free energy state.

The development of the morphology of C–S–H in cement paste most closely resembles the pattern shown by triclinic C_3S. This is at first surprising since not only are the polymorphs different, but with respect to composition TC_3S is the purest sample and cement the most complex, with the probability of interference from reaction of other components present. It is not known whether the MC_3S in cement would show the same hydration characteristics if it was extracted from the mixture and studied in isolation in the same manner as the three C_3S samples. Clearly, an efficient separation process which would preserve surface properties would be needed to carry out such experiments. It is likely that reactivity depends less on crystal structure and more on the exact method of preparation.

Odler and Schüppstuhl [20] have shown that production conditions and ageing can greatly affect the duration of the induction period and rate of heat evolution. They found that fast cooling after firing and fine grinding shortened the induction period, with the total elimination of the induction period for the finest ground sample. Long storage and doping of the sample with Al_2O_3 both considerably lengthened the induction period. From extensive studies of the reactivities of C_3S containing impurities, and of pure C_3S samples which have undergone different

thermal treatments and natural ageing, Fierens [21] has concluded that surface defects introduced by any method are primarily responsible for the wide range of observed reactivities. On balance it appears that although the different polymorphic forms of C_3S studied here are seen to produce distinguishable early hydration products, the question of the relationship between crystal structure and reactivity remains unsolved. Preparative conditions, particle size, impurity levels and the occurrence of surface defects or active sites may be of more importance in determining the hydration behaviour of C_3S. Nevertheless, ultimately all the C_3S samples give hydration products which appear the same. Minor compositional differences which cause significant variations in the early hydration rates or mechanisms, appear to have little long term effect on the morphology.

4. Conclusions

A sequence of reaction steps in the microstructural development of the hydration products of triclinic and trigonal C_3S polymorphs has been identified, but a monoclinic sample has been found to display a somewhat different mechanism. In each case there is initial C–S–H film formation on the C_3S surface but the subsequent rupture of this coating is by lifting and peeling of sheets of material in the monoclinic case, and by random eruption of needle-like outgrowths in the triclinic and trigonal samples. Ultimately all three samples appear identical with thin sheet like C–S–H bridging the perpendicularly radiating outgrowths. Each stage in the reaction sequence can be correlated with conduction calorimetry data, and a model of hydration which considers the mechanism of space filling, in particular during stage III, can account quantitatively for the degree of hydration observed at the end of this stage.

Acknowledgements

The authors wish to thank Dr G. K. Moir of Blue Circle Industries for providing the C_3S samples and conduction calorimetry traces.

References

1. J. SKALNY, I. JAWED and H. F. W. TAYLOR, *World Cem. Technol.* **9** (1978) 183.
2. J. SKALNY and J. F. YOUNG, 7th International Congress on the Chemistry of Cements, Vol. I, Paris, 1980, p. II–1.
3. H. M. JENNINGS, B. J. DALGLEISH and P. L. PRATT, *J. Amer. Ceram. Soc.* **64** (1981) 567.
4. S. DIAMOND, in Proceedings of the Conference on Hydraulic Cement Pastes: Their Structure and Properties, Sheffield, 1976 (Cement and Concrete Association, Slough, England, 1976) p. 2–30.
5. J. W. JEFFERY, *Acta Crystallogr.* **5** (1952) 26.
6. N. I. GOLOVASTIKOV, R. G. MATVEEVA and N. B. BELOV, *Kristallografiya* **20** (1975) 721.
7. M. REGOURD, *Bull. Soc. Franc. Mineral Crist.* **87** (1964) 241.
8. I. MAKI and S. CHROMY, *Cem. Concr. Res.* **8** (1978) 407.
9. P. GOURDIN, E. DEMOULIAN, F. HAWTHORN and C. VERNET, 7th International Congress on the Chemistry of Cements, Vol. II, Paris, 1980, p. I223–228.
10. J. E. BAILEY and D. CHESCOE, *Proc. Brit. Ceram. Soc.* **28** (1978) 165.
11. W. LERCH and R. H. BOGUE, *J. Res. Nat. Bur. Stand.* **12** (1934) 645.
12. T. HARADA, M. OHTA and S. TAKAGI, *J. Ceram. Soc. Jpn.* **86** (1979) 195.
13. G. YAMAGUCHI, K. SHIRASUKA and T. OTA, Highways Research Board Symposium Structure of PC Paste and Concrete SR90, 1966, p. 263.
14. G. L. VALENTI, V. SABATELLI and B. MARCHESE, *Cem. Concr. Res.* **8** (1978) 61.
15. R. A. THOMPSON, D. C. KILLOH and J. A. FORRESTER, *J. Amer. Ceram. Soc.* **58** (1975) 54.
16. R. ALDOUS, *Cem. Concr. Res.* **13** (1983) 89.
17. *Idem, ibid.* in press.
18. S. BRUNAUER, *Amer. Sci.* **50** (1962) 210.
19. D. D. DOUBLE, A. HELLAWELL and S. J. PERRY, *Proc. Roy. Soc. London* **A359** (1978) 435.
20. I. ODLER and J. SCHÜPPSTUHL, *Cem. Concr. Res.* **11** (1981) 765.
21. P. FIERENS, *Cemento* **75** (1978) 195.

Received 21 March
and accepted 30 March 1983